

THREE-DIMENSIONAL NEAR WALL FLOW PHENOMENA OF A TANDEM CASCADE

T. Frey - M. Böhle

TU Kaiserslautern, Institute of Fluid Mechanics and Fluid Machinery, Kaiserslautern, Germany,
thomas.frey@mv.uni-kl.de, martin.boehle@mv.uni-kl.de

ABSTRACT

The two dimensional flow in tandem cascades has often been performed in the open literature. The suggestion is that tandem blades may be superior to single blades, especially for large turning angles. For tandem cascades with a low aspect ratio the losses that are generated at the wall are very important. But up to now less information about the flow structure near the sidewall are available.

Based on current numerical and experimental investigations, the present paper reports on the influence of a tandem cascade configuration on the wall induced losses in an axial compressor. The examinations are performed with a tandem cascade turning the flow from approximately 50° at a Reynolds number of $Re_l = 8 \cdot 10^5$. The load split is 50%. The profiles are NACA65 with circular camber lines. It was designed using empirical correlations of Lieblein and Lei. One goal of the paper is to check the applicability of the criteria of Lei for tandem cascades which was originally developed for single cascades. Therefore the forward blade was designed so that corner stall occurs according to the criteria of Lei.

As the numerical simulations show, the effect of corner stall is suppressed in the design point. The flow phenomena and the comparison of the losses from two-dimensional flow and three-dimensional flow shows, that the main losses of a tandem cascade are generated at the sidewall. The losses are dependent on the configuration of the blades.

NOMENCLATURE

| | | | |
|--------------------------------------|--|--------------------|---|
| c | velocity magnitude | Ma | Mach number |
| d | max. blade thickness | $PP = \frac{s}{t}$ | percent pitch of aft airfoil leading edge relative to spacing |
| h | blade height | Re | Reynolds number |
| i | incidence angle | Tu | turbulence intensity |
| l | chord length | β | flow angle with respect to axial direction |
| p_t | stagnation pressure | $\Delta\beta$ | deflection angle |
| s | pitchwise spacing between forward airfoil trailing edge and aft airfoil leading edge | ζ | stagnation pressure loss coefficient |
| t | cascade pitch | μ | axial velocity ratio |
| Δx_1 | axial distance between aft airfoil leading edge and forward airfoil trailing edge | λ | stagger angle |
| Δx_2 | axial distance between forward airfoil leading edge and aft airfoil trailing edge | σ | solidity |
| AB | aft blade | φ | camber angle |
| $AO = \frac{\Delta x_1}{\Delta x_2}$ | axial overlap of tandem airfoils | Subscripts | |
| D | Lei diffusion parameter | 11 | in front of forward airfoil |
| DF | Lieblein diffusion factor | 12 | behind forward airfoil |
| FB | forward blade | 21 | in front of aft airfoil |
| | | 22 | behind aft airfoil |

INTRODUCTION

In order to minimize the fuel consumption of a turbomachinery the power density and efficiency have to be increased. An increasing of the power density can be achieved by reducing the number of stages of a machine. In order to achieve the same pressure rise with a smaller number of stages the deflection of the single stages must be increased. Usually a higher deflection causes higher pressure losses. So the efficiency can only be increased if the blades realize high deflections with low pressure losses. The advantages of tandem cascades, i.e. compressor stages in which the deflection is taken in two divided sections, in comparison to single cascades for flow deflections greater than 45° are often described in the literature (Railly & El-Sarha, 1965-1966, Wu et al., 1985, Roy, B. & Saha, U.K., 1995, Canon-Falla, G.A., 2004, McGlumphy, 2008). The reason is that at the leading edge of the rear profile a new thin boundary layer exists. For the remaining deflection therefore the risk of boundary layer separation is smaller.

The subject of the investigations until now was the two-dimensional flow and the interaction between the forward and aft airfoil. There are results from a variety of theoretical and experimental investigations of incompressible and compressible flows.

A basic work was done by Ohasi (1958). He performed numerical and experimental investigations with NACA 0010, NACA 4410 and NACA 8410 profiles at Reynolds numbers of $2 \cdot 10^5$. The result of his theoretical investigations was that minimal losses occur when each blade row causes the same change in pitchwise direction. This roughly corresponds to a load split of 50%. Due to the comparison of tandem cascades and single cascades with the same deflection he worked out a limit where tandem cascades generate fewer losses than single cascades. This limit is dependent on both the deflection angle and the angle of attack. The effect of the relative position of the individual tandem blades was examined experimentally. Ohasi found that the rear blade must be located in the non-detached, undisturbed flow on the pressure side of the forward blade. Different distances between the blades in axial direction, however, had no significant effect on the loss incurred. The results were trend setting for a number of scientists who studied the flow in tandem cascades. In good agreement with Ohasi's findings are the experimental results of Railly & El-Sarha (1965-1966). Wu et al. (1985) published a correlation between best overlap and best displacement of the forward and aft-cascade for minimal flow losses according to their measurements with DCA-profiles at moderate Mach numbers ($M \approx 0.3$). Their correlation is in good agreement with the results of Bammert and Staude (1970). They determined the optimal configuration of the tandem cascades with a potential theoretical calculation method which is valid for all tandem cascades. The interference of the blade rows may cause a 10-18% lower pressure loss than the individual blades without mutual interference if the pitchwise spacing is appropriate. The percent pitch is also dependent on both the deflection angle and the angle of attack. Regarding the axial overlap of the front and rear blade row all the previously considered publications are also consistent with the work done by McGlumphy (2008). As a rule it can be concluded that neither a positive nor a negative axial overlap is advantageous in order to reduce flow losses with some small exceptions (see Bammert and Staude, 1970). McGlumphy (2008) determined the flow losses of 2D-flows in tandem cascades consisting of NACA65 profiles by CFD-calculations. He depicted the flow losses of single airfoil cascades and tandem cascades in dependence of the Lieblein's diffusion number DF . For large diffusion numbers DF tandem cascades are superior to single cascades and have a larger incidence range for small flow losses. McGlumphy's results can be listed as follows:

1. For large turning angles ($>45^\circ$) a tandem cascade is better than a single airfoil cascade concerning the flow losses.
2. The blades must be arranged as it is shown in Fig. 1. The dimensions s and Δx_1 must be chosen conveniently.
3. An overlap is not advantageously. Exceptions are mentioned by Bammert and Staude (1970).
4. The load split has an extreme influence on the flow losses.

Today, there is a common agreement with regard to axial overlap and percent pitch. Furthermore there are statements to the aerodynamic load split whereby the load split was only varied by modifying the camber and the stagger angle of the profiles but not by modifying the length of the single profiles. Information about the influence of the profile length on the performance of a tandem cascade is missing. All the previous mentioned literature with the exception of the work of McGlumphy (2008) only deal with the two-dimensional flow in tandem cascades. So the two-dimensional flow parameters of tandem cascades are well known. The work of McGlumphy's contains less information about the 3D-flow structure and the load split which is fundamental for the design of tandem cascades. In the work of Schluer, Böhle, Cagna (2009) the numerical examinations are restricted on the load split and no experimental data are available.

For cascades with low aspect ratio the regions where nearly two-dimensional flow conditions can be found are small. Due to the influence of loss that is generated at the endwall is significant. The authors of the literature above even knew that the performance of a tandem cascade decreases because of the three-dimensional effects but until now these flow structures have never been subject of research.

Lei, Spakovszky (2006) reported about a criterion for corner stall. Corner stall is defined as reverse flow on both the blade surface and sidewall. This criterion, which is actually only valid for single cascades, is applied for tandem cascades in this contribution. It continues the proceeding of the work done by Schluer, Böhle, Cagna (2009). Numerical and experimental examinations on the three-dimensional flow in the hub region of a tandem cascade are done. All calculations are conducted as incompressible ($Ma=0.18$). The tandem cascade consists of NACA65 profiles turning the flow from 50° to approximately 0° . The influence of the percent pitch $PP = \frac{s}{t}$ at constant load split

$$LS = \frac{DF_1}{DF_1 + DF_2} \quad (1)$$

on the flow losses and the flow topology is examined by wind tunnel experiments and 3D-CFD simulations. The main emphasis lies on the description of the three dimensional flow structure with focus on hub corner stall.

DESIGN OF THE EXAMINED TANDEM CASCADE

The tandem cascades in this contribution were designed in several respects. They should provide information about the influence of the percent pitch on the flow structure near the sidewall of tandem cascades and about the applicability of the criterion for hub corner stall on tandem cascades. The blade rows of the tandem cascade consist of NACA65 profiles with circular camber lines because a large number of experimental data are available. The cascade should deflect the flow from $\beta_{11} = 50^\circ$ to $\beta_{22} = 0^\circ$ at a Reynolds number of $Re = 8 \cdot 10^5$. The Reynolds number for the whole cascade is defined as follows:

$$Re = \frac{c_{11} \cdot l_{eff}}{\nu} \quad (2)$$

According to Johnsen, Bullock (1965) the stagger angle and the camber angle of a NACA65 profile arise as a result of the solidity, the relative thickness and the target values of the flow angle.

Assuming that the outflow angle of the forward blade row is equal to the inflow angle of the aft blade row both the Lieblein diffusion factor and the Lei diffusion parameter can be calculated for the blade rows on basis of this data. The Lieblein diffusion factor

$$DF_1 = 1 - \frac{\cos \beta_{11}}{\cos \beta_{12}} + \frac{\cos \beta_{11}}{2} \cdot \left(\frac{t}{l_1}\right) \cdot (\tan \beta_{11} - \tan \beta_{12}) \quad (3)$$

is a measure for aerodynamic load of the two-dimensional flow. DF is written for the forward cascade and can be applied for the aft cascade and the whole cascade by using the corresponding parameters. The Lei diffusion parameter

$$D_1 = \frac{t}{l_1} \cdot \left[1 - \left(\frac{\cos \beta_{11}}{\cos \left(\lambda_1 - \frac{\varphi_1}{2} \right)} \right)^2 \right] \cdot (i_1 + \varphi_1)^* \quad (4)$$

is a measure for the aerodynamic load of the three-dimensional flow. D is also written for the forward blade row and can be applied for the aft blade row and the whole cascade using the corresponding parameters. All angles in equation (3) and (4) are in degree with respect to the factor $^*(i + \varphi)$ in equation (4) which is in radians. The diffusion parameter D and the diffusion factor DF of each blade row are dependent on the flow angles and the spacing ratio. The diffusion factor for the whole cascade is just dependent on the spacing ratio of the whole cascade because the deflection was already fixed. In order to keep the value of DF_{OV} beneath the critical value of 0.6 the value for t/l_{eff} was set to 0.6. McGlumphy (2008) worked out the ideal parameters for the axial overlap AO and the percent pitch PP for the two-dimensional flow. According to his work a configuration with $AO = 0\%$ and $PP = 90\%$ generates minimum loss. The numerical results of Schluer, Böhle, Cagna (2009) show that a load split of $LS = 50\%$ generates minimum losses for the two-dimensional flow and for the three-dimensional flow. So these parameters were applied for the investigation. In order to get an overview of all the tandem cascades that meet the mentioned requirements an iterative calculation method based on the NACA 65 data was created. The corresponding Lieblein diffusion factors and Lei diffusion parameters are shown as a function of the spacing ratio of the forward blade row in Fig. 2. As a criteria for the occurrence of corner stall serves the diffusion parameter D . According to Lei, Spakovski (2006) corner stall is expected for values of $D = 0.4 \pm 0.05$.

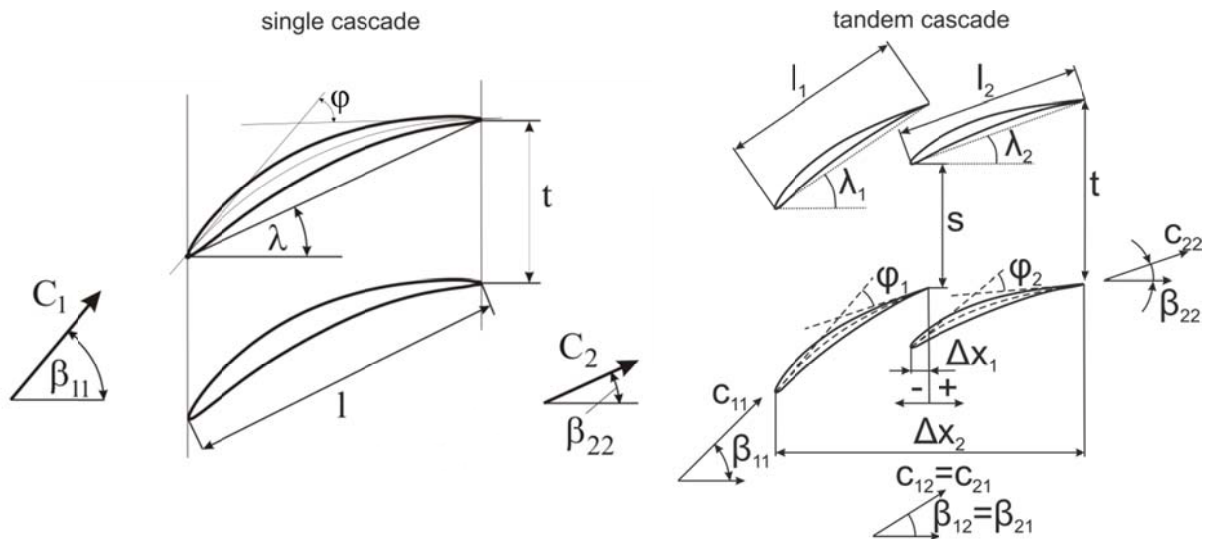


Figure 1: Parameters at single and tandem cascade

As shown in Fig. 2 the Lei diffusion parameter of the forward blade row D_1 exceeds the critical value for big spacing ratios of the forward blade row while the value for the aft blade row D_2 remains uncritical over the entire range. The design of the examined tandem cascade was selected so that corner stall is expected with regard to equation (4) for the forward blade row.

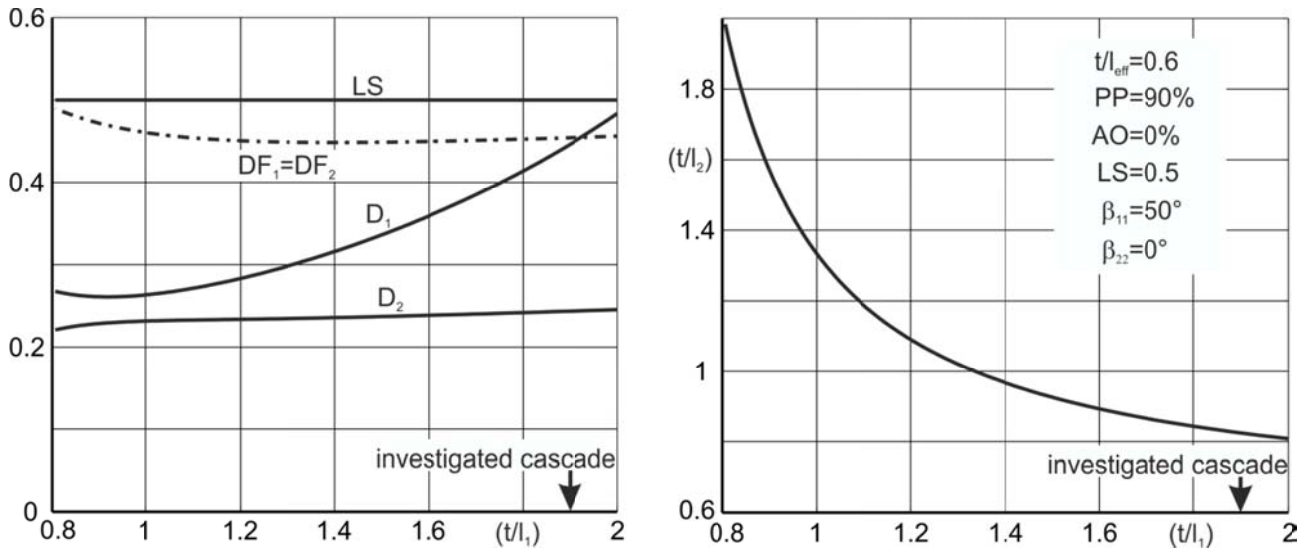


Figure 2: Lieblein diffusion factor and Lei diffusion parameter as a function of the spacing ratio

The corresponding parameters of the selected tandem cascade are given in Table 1 on the left. The same blade rows were used to determine the influence of the percent pitch. Therefore the aft blade row was moved relative to the forward blade row in pitchwise direction so that the cascade had a percent pitch $PP=70\%$. The corresponding parameters are given in Table 1 on the right.

| Parameter | PP=90% | | | PP=70% | | |
|---------------|---|--------|-----------------|---|--------|-----------------|
| | FB | AB | Overall cascade | FB | AB | Overall cascade |
| DF | 0.4547 | 0.4547 | 0.5775 | 0.4547 | 0.4547 | 0.5775 |
| D | 0.4235 | 0.2330 | 0.3577 | 0.4235 | 0.2330 | 0.3737 |
| d/l | 0.1 | 0.1 | | 0.1 | 0.1 | |
| Δx_1 | | 0 | | | 0 | |
| s [mm] | | 103.5 | | | 80.5 | |
| t [mm] | 115 | 115 | 115 | 115 | 115 | 115 |
| l [mm] | 60 | 140 | 191.7 | 60 | 140 | 184.7 |
| t/l | 1.9167 | 0.8214 | 0.6 | 1.9167 | 0.8214 | 0.6226 |
| φ [°] | 31.9 | 47.1 | 65.2 | 31.9 | 47.1 | 65.2 |
| λ [°] | 40.6 | 15.0 | 19.4 | 40.6 | 15.0 | 12.7 |
| | $\beta_{11} = 50^\circ$ $\beta_{12} = \beta_{21} = 37.4^\circ$ $\beta_{22} = 0^\circ$ | | | $\beta_{11} = 50^\circ$ $\beta_{12} = \beta_{21} = 37.4^\circ$ $\beta_{22} = 0^\circ$ | | |

Table 1: Parameters of the examined tandem cascade

The dimensions of the cascade correspond with the dimensions of the cascade wind tunnel. Although the forward blade row has a small spacing ratio with respect to the aft blade row the Lieblein diffusion factor is the same. The values of the Lieblein diffusion factors are smaller than the critical value of 0.6. From this reason two-dimensional separation is not expected in the design point. The change of the percent pitch only has influence on the spacing ratio and the Lei diffusion parameter of the overall cascade. The Lieblein diffusion factor is not affected because the spacing ratio included is calculated in a different manner for the whole cascade.

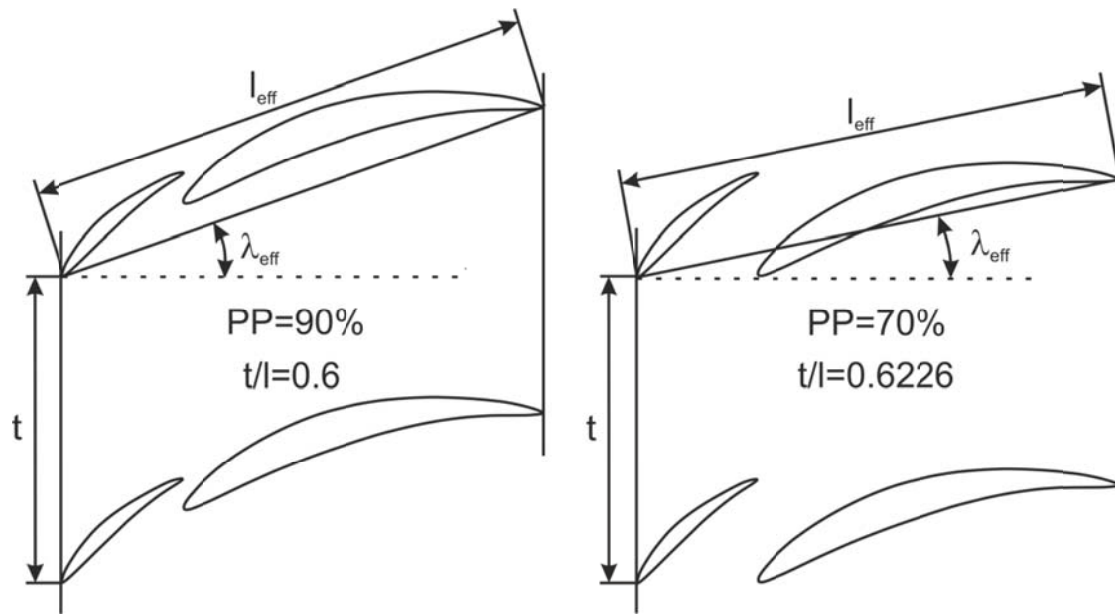


Figure 3: Cascades with different percent pitch

NUMERICAL METHOD

The flow domain for the numerical investigations was adjusted to the local boundary conditions of the used wind tunnel. It was created so that both symmetry boundary conditions and periodic boundary conditions were applied. The dimensions of the domain correspond to those of the cascade wind tunnel. For each tandem cascade two-dimensional and three-dimensional flow domains were created. The 3D domains are extrusions of the 2D domains. Using the software package Icem CFD from ANSYS (mesh generator from FLUENT Software package) the flow domains were discretized with block-structured hexahedral grids. The refinement of the grids was adjusted to the requirements of the software for the numerical simulations and the used turbulence model. The numerical simulations were done with the software package ANSYS Fluent 13. As turbulence model the Spalart Allmaras model has been selected. It was designed for aerospace applications and is increasingly being used in turbomachinery applications (FLUENT Software package). It is characterized by its robustness and gives good results in the calculation of boundary layers and boundary layer thicknesses. It is also suitable for the calculation of wakes and mixed flows of wakes (Schmidt, 2011). The Spalart Allmaras model is in its origin form a low-Reynolds-number one-equation model. The viscous region of the boundary layer must be resolved properly ($y^+ < 3$). In this case the viscosity-dominated sublayer is directly calculated using the laminar stress-strain relationship (FLUENT Software package). For meshes with $y^+ > 30$ Fluent automatically uses wall functions. From this reason two different refinements were applied for the three-dimensional calculations. One flow domain that is applied uses wall functions ($y^+ \sim 100$, 2 million cells) and one flow domain is properly resolved ($y^+ < 3$, 5.4 million cells). This should show if the wall function grid is able to represent the real flow structure.

Figure 4 shows the 3D flow domain with the corresponding boundary conditions. The inflow boundary conditions at the “inlet” were determined by measurements. The velocity profile of the inflow was measured at the cascade wind tunnel with a calibrated five-hole probe. A good approach for the velocity in the boundary layer of the inflow is obtained by the 1/7-power law over a boundary layer thickness of 40mm with 2/21 as well exponent (SEE Fig. 5). The isotropic turbulence intensity was measured with a calibrated hot wire anemometer “StreamLine research CTA system” and the corresponding software “StreamWare Vol. 3” from Dantec. At the required flow velocity the turbulence intensity is $Tu=0.2\%$. The turbulence intensity has been established in the flow simulations.

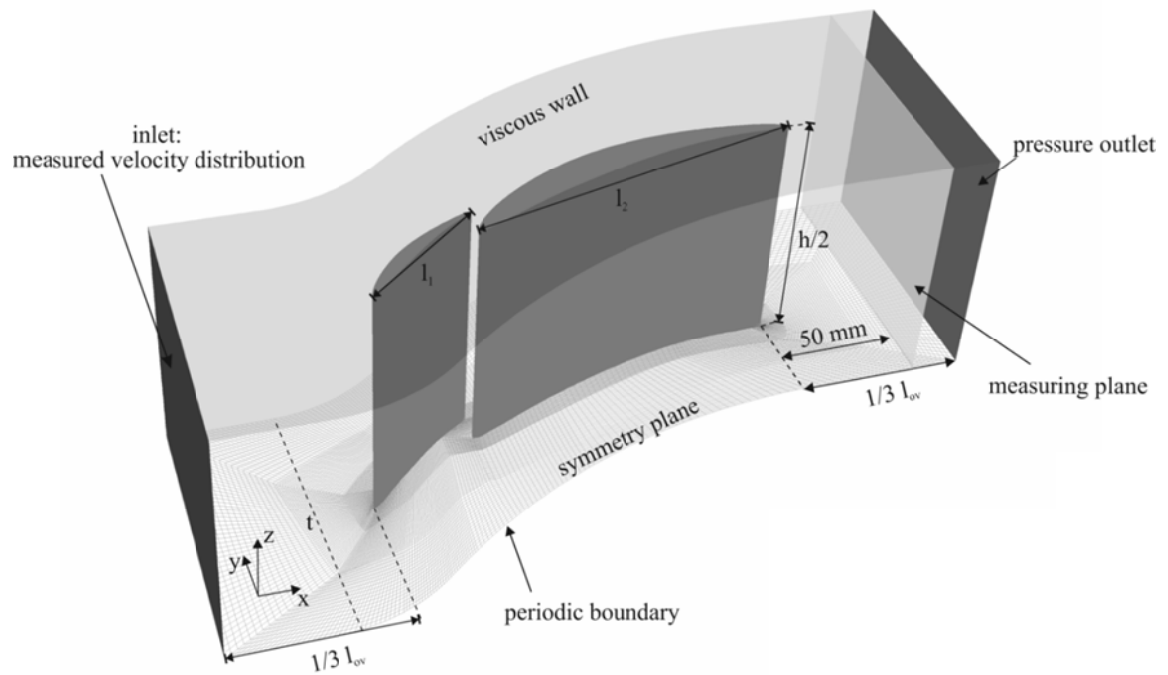


Figure 4: Flow domain with boundary conditions

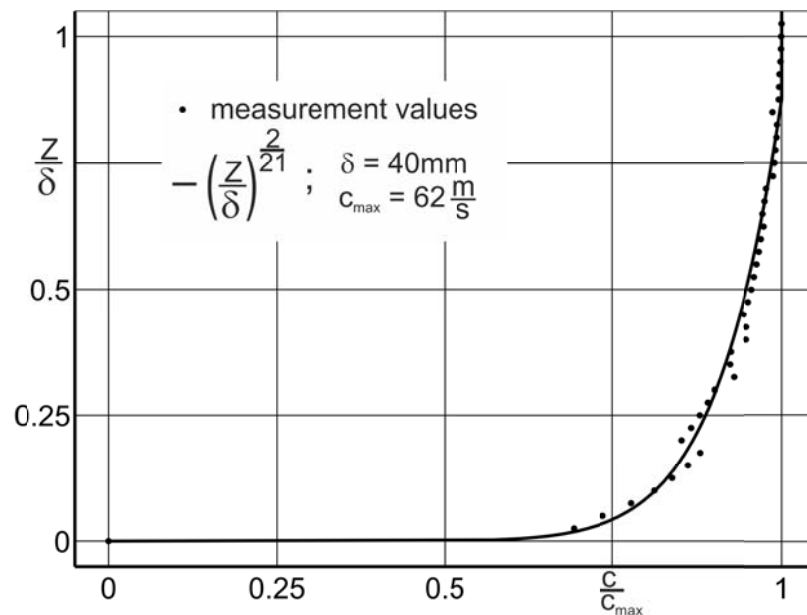


Figure 5: Measured boundary layer profile of the cascade wind tunnel

EXPERIMENTAL SETUP

The experimental investigations are carried out at a cascade wind tunnel. It consists of an inflow nozzle (inner diameter 710mm, length 1575mm), a frequency-controlled axial-flow compressor (diameter 600mm, $\dot{V} \sim 45000 \frac{\text{m}^3}{\text{h}}$, $\Delta p \sim 1000\text{Pa}$), a honey-comb grid (comb distance 9mm, comb thickness 0.3mm, length 160mm) to take the swirl produced by the compressor out of the flow, an acceleration nozzle (length 1500mm, inflow diameter 705mm, outflow cross section 500mm height x 200mm width), a smooth segment with unchanged cross section (length 600mm) and a test section. A picture of the cascade wind tunnel can be seen in Figure 6. In front of the test section two frequency controlled side channel compressors are installed in order to suction the boundary layers

of the upper and lower limit of the smooth section. They are also used to adjust the inflow angle of the test section and to realize periodic conditions. The reference values for the stagnation pressure and the static pressure are measured with a Prandtl tube in front of the cascade. It is positioned in the center of the inflow cross section. The test section is rotatable in order to realize different angles of attack. The side walls on which the blades are attached are made of glass so that oil-flow pictures are visible from the outside and can be photographed. The blades themselves were milled from aluminium. In a distance of 50mm behind the aft blades trailing edge the flow conditions are measured by a calibrated five-hole probe. The five-hole probe is attached to a computer-controlled traversal. It can be adjusted behind the test section in an arbitrary distance and angle. So for the measurements it is parallel to the outflow plane so that the tip of the five-hole probe is in the measurement plane. The five-hole probe has a length of 250mm and a tip diameter of 1.6mm. Measurements can therefore be carried out up to a distance of 3mm to the sidewalls. Five-hole probe measurements are performed in the entire measurement plane. The stepsize in pitchwise direction is 1mm. Perpendicular to the wall the step size of the measurement series is adjusted to the gradients of the flow parameters.

Furthermore, measurements of the blade pressure distribution are performed for the forward and aft blade at midspan and in a distance of 10% of each chord length to the sidewall. From the blade pressure distributions the stall indicator is calculated according to Lei, Spakowszky, Greitzer (2006).

Experimental oil flow pictures are created using a fluorescent fluid. The fluid is sprayed onto the blades and the side wall before the cascade wind tunnel is turned on. Then it slowly runs as a result of friction and leaves traces of the wall stream lines. The resulting picture can be photographed.

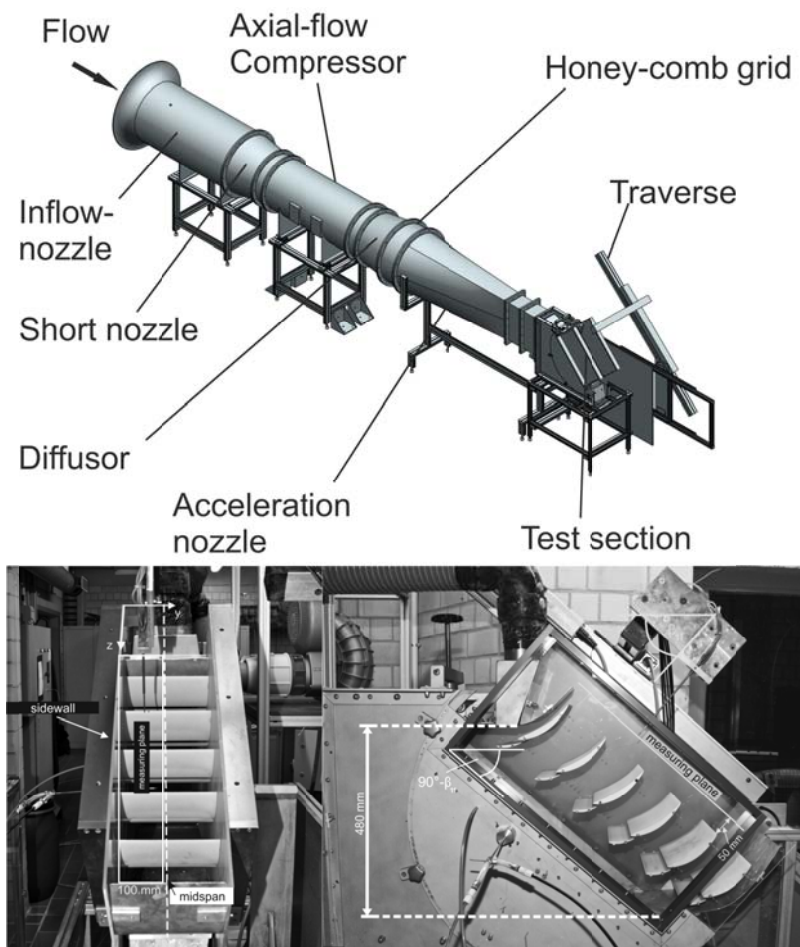


Figure 6: Cascade wind tunnel

RESULTS AND DISCUSSION

The numerical simulations may reflect the flow conditions and the flow structure on the side wall and on the suction side of the blades very well. However, the flow domain in the wall region must be resolved properly ($y^+ < 3$). Flow simulations in which the flow in the boundary layer is calculated using wall functions could only approximate the actual flow structure for angles of attack from 40° to 50° . For higher angles of attack they were completely wrong. At cascades with high deflection the use of wall functions should be avoided. The numerical results in this contribution are from CFD simulations with properly resolved grids ($y^+ < 3$).

The results of the two-dimensional flow simulation are in good agreement with the data from the literature. A tandem cascade configuration with a small gap between the forward and aft blade row (PP=90%) causes fewer losses than a configuration with a large gap (PP=70%). This is also confirmed by the currently available measurements. The mass averaged pressure loss coefficients are shown in Fig. 7 for the two-dimensional as well as for the three-dimensional flow. The mass averaged pressure loss coefficient is calculated by

$$\bar{\zeta} = \frac{\sum \zeta_i \cdot \rho_i \cdot \vec{c}_i \cdot \vec{A}_i}{\sum \rho_i \cdot c_i \cdot A_i} \quad (5)$$

$$\zeta_i = \frac{p_{t,i} - p_{t,11}}{\frac{\rho_{11}}{2} \cdot c_{11}^2}. \quad (6)$$

The index i is the local cell value of the numerical results and the local measurement point value, respectively. A_i is the size of the local cell outflow plane and the size of the local measurement point grid size.

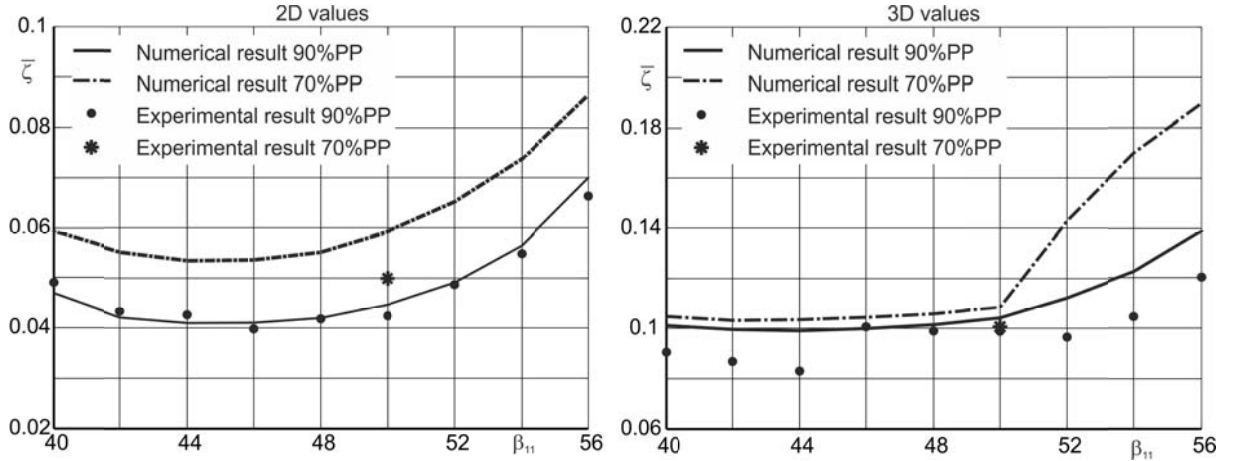


Figure 7: Mass averaged pressure losses

The mass averaged three-dimensional experimental values are not absolutely correct because the flow angles exceeded the range of validity of the five-hole probe calibration in regions of high pressure losses. Therefore they can only serve as a rough guide. The numerical results show that the mass averaged pressure losses of the three-dimensional flow through the tandem cascades is almost identical for angles of attack smaller than 50° . For angles of attack greater than 50° the losses of the 70% PP configuration rise more than for the 90% PP configuration. It can be seen on the flow structure in the region near the side wall where losses occur and how they spread. Within the side wall boundary layer the pressure force acting on the fluid particles are no longer in equilibrium with the force of inertia. Due to a cross-flow from the blades pressure side to the suction side is generated. This cross-flow meets the surface of the next blades suction side and turns from the side

wall in the direction of the flow channel center. The flow converges on the blades suction side with the flow that was already crossing the blades suction side. This creates a three-dimensional separation line on the blades suction side. Along this separation line losses are generated. Additional three-dimensional separation lines are generated at the side wall behind the blade trailing edges. In these lines the flow of the cross-flow converges with the flow coming from the pressure side of the blades and separates from the side wall. The resulting losses connect the wakes of the individual blades at the side wall. This can be seen in Fig. 8.

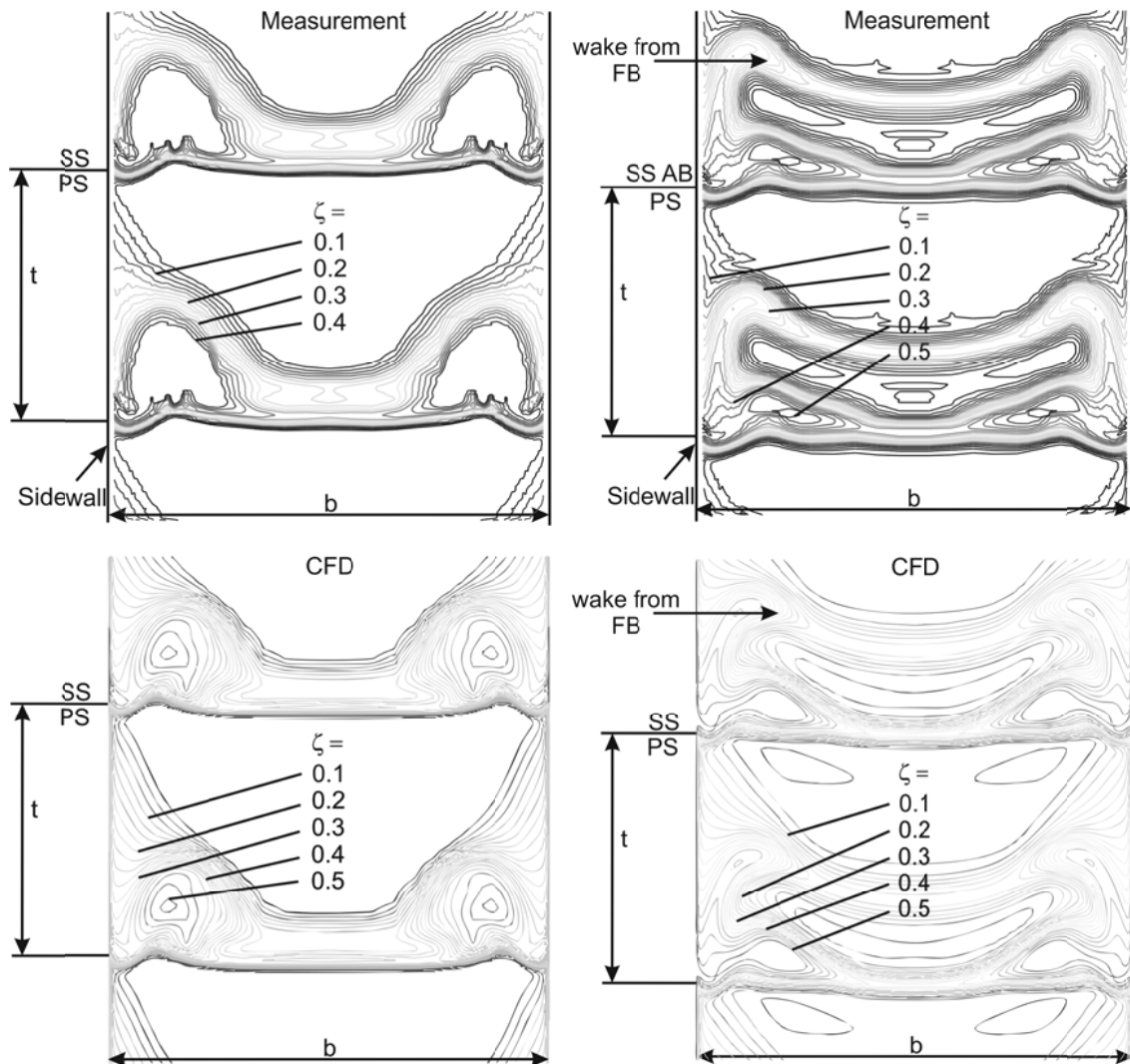


Figure 8: Contours of local ζ -values in the measurement plane. Left side: 90% PP, right side 70% PP, $\beta_{11} = 50^\circ$

The suction side of the aft blade row is always loaded by those losses that are generated along the separation line between the forward blade row and the aft blade row. The consequence of this is corner stall at the aft blade row, although the diffusion parameter is not critical. So corner stall at the aft blade row occurs for both tandem configurations and for all investigated angles of attack between 40° and 56° . The diffusion parameter is therefore not valid as indicator for the occurrence of corner stall at the aft blade row of tandem cascades.

The flow through the forward blade row is nearly independent of the position of the aft blade row with respect to the forward blade row. In accordance with the criterion by Lei, Spakovszky, Greitzer (2006) corner stall occurs in the forward blade row. The numerical results show this starting at angles of attack of 52° . The experimental oil-flow pictures show corner stall starting at angles of attack of 50° (SEE Fig. 9).

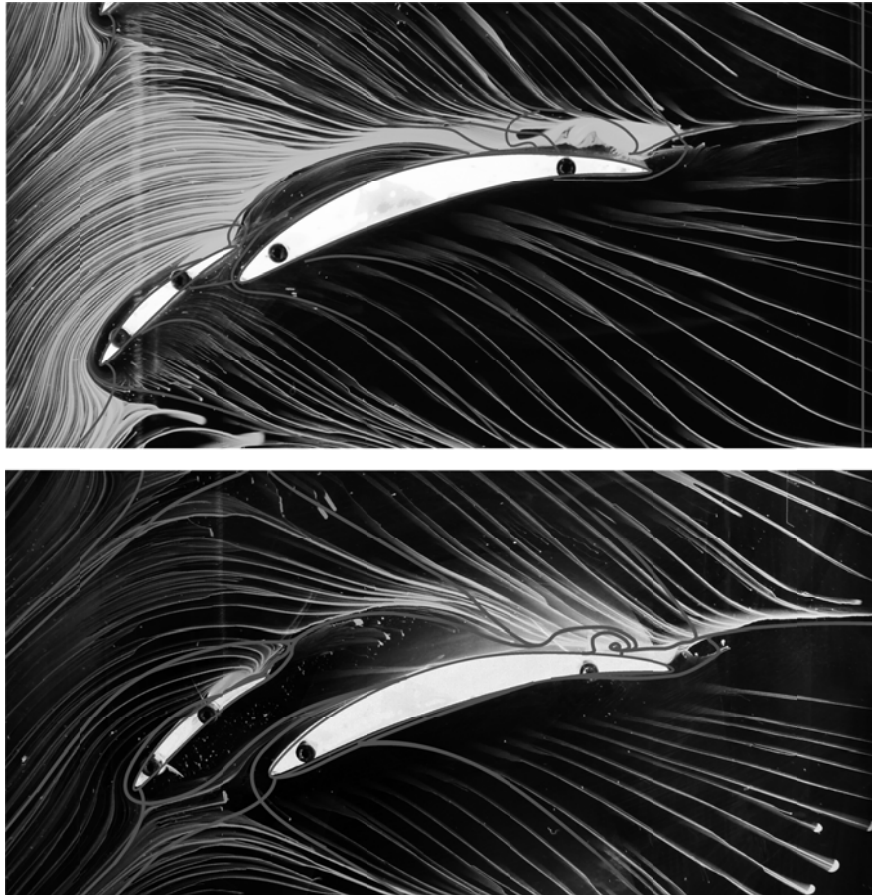


Figure 9: Experimental oil-flow picture superimposed by the numerical results of the flow structure (grey lines). Upper image: 90% PP, lower image: 70% PP, $\beta_{11} = 50^\circ$

Corner stall causes additional losses. The occurrence of corner stall in the forward blade row also affects the flow structure in the aft blade row. The flow from the forward blade row pressure side is influenced by the occurrence of corner stall so that its positive influence on the aft blades suction side is minimized. The size of the corner stall at the 70% PP configuration is slightly larger. The reason could be the influence of the two-dimensional flow behavior. The overall losses therefore increase faster for angles of attack of more than 50° . For angles of attack smaller than 50° , where corner stall is not present, the bigger gap of the 70% PP configuration is advantageous to the 90% PP configuration in the region of the wall because more pressure side fluid from the forward blade row meets the suction side of the aft blade row. As a result the boundary layer from the aft blade row is pushed downstream. The corner stall region in the aft blade row is therefore smaller. This can be seen in Figure 10 which shows the flow structure of the tandem cascades for angles of attack of 50° . One more advantage of a larger gap is that the losses behind the cascade are located near the wall with the exception of the wakes of the blades. For the 90% PP configuration the losses fuse to a large loss zone behind the cascade (SEE Fig. 8). The outflow angles in this loss zone exceed the validity of the five-hole probe calibration. From this reason the ζ -values are only shown up to $\zeta=0.4$.

CONCLUSIONS

Two tandem cascades with different percent pitch were analyzed with regard to their loss generation in the region near wall (hub region). The validity of an indicator for the occurrence of corner stall was examined for tandem cascades. Additionally, this paper gives information about the

influence of the individual blade length in tandem cascades. The investigated tandem cascades were designed for a deflection of the flow from $\beta_{11} = 50^\circ$ to $\beta_{22} = 0^\circ$. The angle of attack was varied from $\beta_{11} = 40^\circ$ to $\beta_{11} = 56^\circ$.

Numerical and experimental results have shown that the Spalart Allmaras turbulence model can reproduce the flow structure in tandem cascades well if the flow domain is properly refined ($y^+ < 3$). The diffusion parameter according to Lei, Spakovszky, Greitzer (2006) is valid to predict the occurrence of corner stall for the forward blade row of a tandem cascade but it is not valid for the aft blade row. For a load split $LS = 50\%$ the Lei diffusion parameter for the forward blade row increases with the spacing ratio of the forward blade row.

The two-dimensional flow behavior through the tandem cascades is consistent with the data from the literature. A tandem cascade configuration with high percent pitch (PP=90%) causes fewer losses in the two-dimensional flow than tandem cascades with lower percent pitch (PP=70%). In the region near the side wall the configuration with PP=70% has a positive influence on the generated loss if corner stall is suppressed. If corner stall occurs in the forward blade row it has significant influence on the flow through the aft blade row because the generation of additional losses in the aft blade row is favored.

The chord length of the individual blades has influence on the spread of the losses in the direction of the flow channel center. Higher chord length cause that losses spread along three-dimensional separation lines on the suction side of the blades. From this reason blades with nearly same chord length seem to be advantageous in order to avoid the spread of losses.

REFERENCES

- [1] J. McGlumphy (2008): Numerical Investigation of Subsonic Axial-Flow Tandem Airfoils for a Core Compressor Rotor. Blacksburg.
- [2] C. Schluer, M. Böhle, M. Cagna: Numerical Investigation of the Secondary Flows and Losses in a High Turning Tandem Compressor Cascade, European Conference on Turbomachinery-Fluid Dynamics and Thermodynamics, 23-27th March 2009, Graz, Austria
- [3] I.A. Johnson, R.O. Bullock, editors (1965): Aerodynamic Design of Axial-Flow Compressors. NASA SP-36
- [4] V.-M. Lei, Z. S. Spakovszky, E. M. Greitzer: A criterion for axial compressor hub-corner stall. ASME Paper GT2006-91332, 2006.
- [5] Raily, J.W. & El-Sarha, M.E. (1965-66): An Investigation of the Flow through Tandem Cascades. Proc. of Institute of Mechanical Engineers., Vol. 180, Pt. 3F
- [6] Wu, G., Zhuang, B., and Guo, B. (1985): Experimental Investigations of Tandem Blade Cascades with Double Circular Arc Profiles. ASME Paper No. 85-IGT-94
- [7] Roy, B. & Saha, U.K. (1995): Experimental Analysis of Controlled Diffusion Compressor Cascades with Single and Tandem Airfoils. ASME paper 95-CTP-41
- [8] Roy, B., & Saha, U.K. (1995): High Diffusion Cascades for Axial Flow Compressor Applications. Proceedings of 15th Canadian Congress of Applied Mechanics
- [9] Canon-Falla, G.A. (2004): Numerical Investigation of the Flow in Tandem Compressor Cascades. Diploma thesis, Departamento de Ingenieria Macanica, Universidad Nacional de Colombia, written at Institute of Thermal Powerplants, Vienna University of Technology
- [10] FLUENT-Software Package: Centerra Resource Park, 10 Cavendish Court, Lebanon, NH 03766
- [11] H. Ohasi (1959): Theoretical and Experimental Investigations on Tandem Pump Cascades with High Deflection. Ing. Archiv, Bd. 27.
- [12] K. Bammert, R. Staude (1970): Optimization for Rotor Blades of Tandem Design for Axial Flow Compressors. ASME Paper 79-GT-125.
- [13] T. Schmidt (2011): Quantifizierbarkeit von Unsicherheiten bei der Grenzschichtwiedergabe mit RANS-Verfahren. Berlin.